New Protection Wall Against Rockfall Using a Ductile Cast Iron Panel

Diop AMINATA[1], Atsushi YASHIMA[1], Kazuhide SAWADA[1], Eunsu SUNG[1],
Kensaku SUGIMORI[1], and Shoichi INOUE[2]
[1] Department of Civil Engineering, Gifu University
[2] Protec Engineering Co. Ltd

(Received for 30 May, 2007 and in revised from 1 Oct., 2007)

ABSTRACT

In Japan, slope disasters occur due to earthquakes, abnormal weather and inappropriate land development. It is important to identify safe and economical countermeasures against rockfall disasters. We developed a simple, long-lasting and low-cost structure with maximum impact dissipative action when stopping rockfall. In order to simulate rockfall impact, various energies of falling rocks were made to collide with real-scale protection structures. The new type of protection wall against rockfall using a ductile cast iron panel is an efficient barrier and has an effective dissipative function. It also has very good permeability. The structure is flexible and the design and construction can take into account of the natural environment and topographic features.

1. INTRODUCTION

In Japan, the risk of slope disaster is very high because of the geology, weather conditions and the patterns of land use. Rockfall is a continuous threat not only to inhabitants of mountainous regions, but also to roads and railway tracks where areas for natural escarpment or excavation exist. Despite usually involving limited volumes (Rochet, 1987), rockfalls are characterized by high energy and mobility, making them a major cause of landslide fatality. Rockfalls can be triggered by a variety of factors including earthquakes (Kobayashi et al., 1990), rainfall, freeze-and-thaw cycles (Matsuoka and Sakai, 1999) or the progressive chemical weathering of rocks and their discontinuities.

Rockfall, the free movement of stones on steep slopes, occurs when rocks on a slope becomes dislodged and fall down the slope. The falling mass often detaches from a steep cliff along geological planes, cracks and joints. A rockfall may be a single rock or a mass of rocks, and the falling rocks can dislodge other rocks as they collide with the cliff. Boulders fall, roll or bounce down the slope according to the slope angle and surface roughness. In some instances, boulders may also slide down the slope (Matsuo et al. 2002; Ritchie, 1963).

The results of the road disaster prevention survey carried out in 1996 across the whole country revealed a huge number of dangerous slopes in Japan. As a result, 145,500 slopes were identified as needing monitoring, and 56,700 slopes as needing urgent disaster prevention projects. In the case of Gifu Prefecture, which is the target area in this research, 1,882 slopes were identified as needing disaster prevention among 5,000 monitored slopes along 4,200 km of road maintained by the prefectural government. Furthermore, slope disasters have been increasing every year due to earthquakes, which have occurred continuously in recent years, and also the abnormal weather and land development. Efficient countermeasures against dangerous slopes are required to protect human life and property from the danger of rockfall or soil flow at many dangerous slopes in Gifu Prefecture.

The scale of rockfalls is predicted by field surveys, and then the energy can be roughly calculated by using the fall height estimated values. From the rockfall energy levels mentioned in the falling-rocks manual standards, appropriate rockfall protection structures are selected as shown in **Fig.1** (Japan Road Association: Rockfall Countermeasures Manual, 2000). Although it is important that countermeasure works are determined by energy levels, it is also necessary to identify construction methods that respond to various demands, such as lower environment impact, inexpensive construction cost and maintenance.

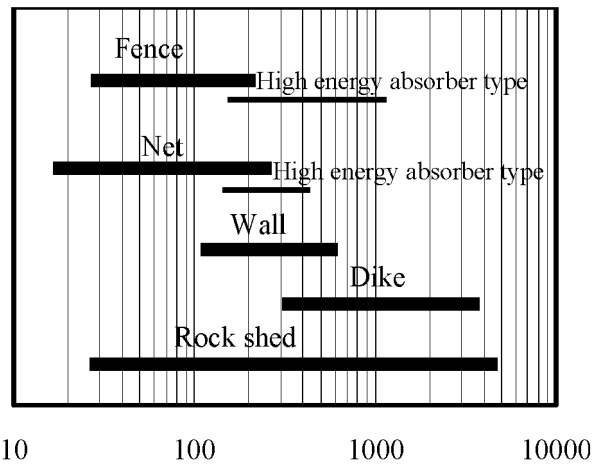

Fig. 1 Choice of protection structures according to the rock fall energy levels

KEY WORDS: Rockfall, Disaster, Protection wall, Ductile cast iron panel, Shock absorber

There are many studies on the stability evaluations of slope and soil flow (Sumi and Yashima, 2000). However, with a limited budget framework and with various environmental problems, disaster prevention programs are not progressing sufficiently.

The most commonly used protection structures against rockfalls are rock sheds, fills, retaining walls, ditches, prevention fences and prevention nets. These structures are commonly placed close to the elements at risk and their role is to intercept and stop the rockfall by transforming kinetic energy to elastic and plastic deformation but also to retain satisfactory performance over time while not requiring much maintenance. In 1990, the distribution of the protection structure types was as follows: 46% for fences, 38% for nets, 14% for walls, 1.3% for rock sheds and 0.7% for other methods (Matsuo et al. 2002). New construction methods against rockfalls have been developed based on the locally prevailing circumstances, the degree of danger and the expected event. These barriers are capable of absorbing energy of up to 3000 kJ within a single rockfall event. Their main idea is not to use a rigid barrier but to stop the rock gradually over a relatively long distance in order to reduce peak load in all barrier's components (Heierli et al., 1981). These flexible barriers need several components such as steel nets supported by cables, posts and braking elements acting together.

In this study, we examined new countermeasures against rockfalls and soil flow using ductile cast iron panels. The objective was to develop a simple, long-lasting and low-cost structure with maximum impact dissipative action when stopping the rockfall. In order to evaluate the performance of different countermeasures, to enhance the comprehension of their mechanical behavior during impact and improve their design and repairing methods, we carried out real-scale field tests.

A ductile cast iron panel of 50 cm in height and 100 cm in length was used. This type of mesh panel has so far been used for riverbed, slope works, etc (Sawada et al, 2005 and 2006).

A wall using ductile cast iron panels has the following advantages:

1) The design and construction take the environment into consideration by using local ground material, and enable vegetation growth. Since local, natural stone can be used as the filling material, a porous structure can be formed and inside water pressure is not accumulated.
2) Compared with steel, ductile cast iron has good durability against salt and acid, and has almost no water retention and environmental pollution. It is also recyclable.
3) Since a wall using a ductile cast iron panel is made from a combination of standardized panels, it can be assembled swiftly. The protection wall using a ductile cast iron panel can be erected in two days; compared to the two weeks for a geogrid-reinforced wall and the one month for a concrete wall.
4) Less care is required for compaction and density when the panel is filled up with boulders compared to a geogrid-reinforced wall.
5) A design, which follows any topography, is possible, and the dissipative process of the impact load takes place easily.
6) A wall using a ductile cast iron panel can be constructed even on soft ground without using a rigid foundation, whereas an excavation and construction of a rigid foundation are necessary in the case of a concrete wall.

2. EXPERIMENTAL METHODOLOGIES

In order to simulate rockfall impact, various energies of falling rocks and imitation rocks were assumed and made to collide with real-scale protection structures using ductile cast iron panels. In this study, three experimental investigations were carried out in 2004, 2005 and 2007 as follows.

2.1 First-step field test

Experiments were carried out in Ibigawacho Quarry in October 2004. Three kinds of loads were allowed to roll and fall down a 17-m high slope at a 45-degree inclination as shown in **Fig. 2**. The loads were made to collide with the rockfall protection walls, which have a ductile cast iron panel frame shock absorbing material. The cast iron spherical falling mass was of 150, 300, 600 mm in diameter, and 0.36, 1.67, and 5.00 kN in weight respectively.

The impact load test was conducted several times with or without panel frame shock absorbing material. **Photo 1** shows the rockfall protection wall, which has panel frame shock absorbing material and **Photo 2** shows a backhoe dropping a rock at the test site.

After assembling the load receptacle stand and rockfall protection wall made of H-type steel, panel frame shock absorbing material was arranged for the test. One unit of the panel frame was (1.0

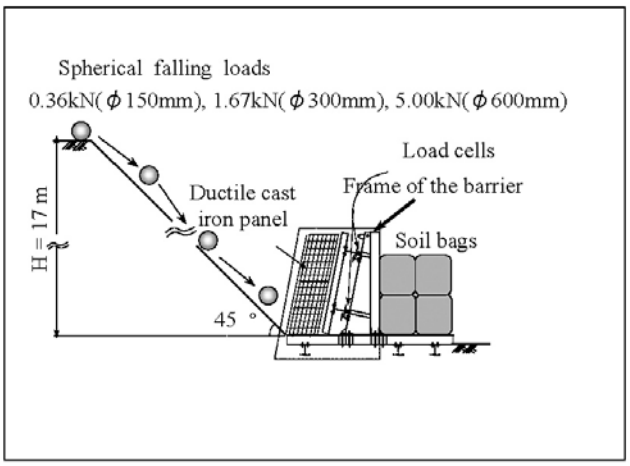

Fig. 2 Outline of the first-step field test

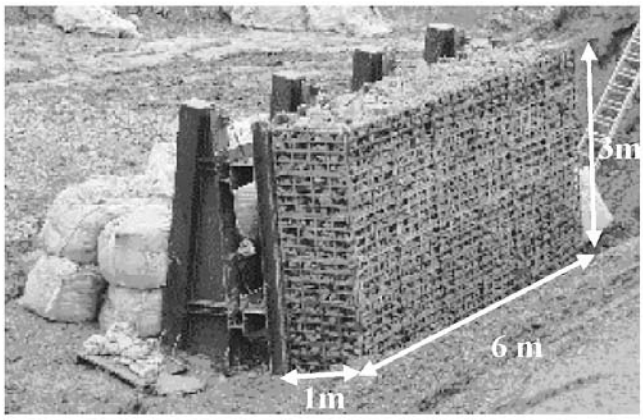

Photo 1 Protection wall using ductile cast iron panel

Photo 2 Backhoe dropping a rock

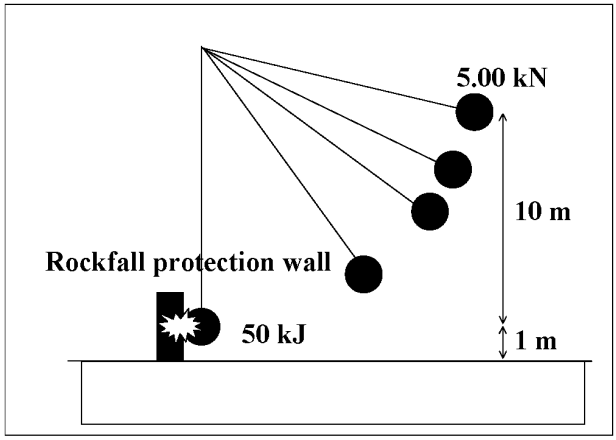

Fig. 3 Outline of the second-step field test

m x 2.0 m x 0.5 m) assembled, then extended to 6.0 m in length, 1.0 m in width and 3.0 m in height (six steps) was installed in front of the load receptacle stand. The framework of the panel was filled up with boulders. The kinetic quantity of the impact load and the involved deformation were measured. Eight sets of load cells were fixed to the load receptacle stand and response loads were measured using a digital dynamic strain meter.

The sampling interval was set to 0.2 ms (5000 Hz), and the measurement time was set to about 3 seconds. For the measurement, several tests were performed under the same conditions. Visual observation and measurements were carried out on the characteristics of the load collision place at the panel frame shock absorbing material, the horizontal movement of the protection wall, and the damage of the panel frame shock absorbing material. Moreover, the falling path of the rock was recorded with a high-speed camera. After that test, the cast iron panel frame was removed, and then a direct impact load test was performed on the protection wall (H-type steel) without panel frame shock absorbing material. Similar dynamic measurements and visual observation were carried out.

2.2 Second-step field test

During the first-step field test, a spherical mass was released to fall down the sloping ground. However, it is difficult to control the impact forces due to friction between the mass and rough sloping ground when falling. For this reason, free fall collision tests were carried out in November 2005 in Kakamigahara (**Fig. 3**). Two cranes were used for the tests. The two cranes lifted a mass of 5.00 kN to a fall height of 11 m, and then dropped the mass as shown in **Photo 3**.

A 3-dimensional accelerometer was connected to the falling load and then the impact force and the energy were computed from the acceleration record, and the displacement (interpenetration condition) of the falling weight at the time of collision.

Each physical quantity is computed using the time series data (sampling frequency 5000 Hz), and the results were compared. The calculation method of each physical quantity is shown first. From the time series data of measured falling load acceleration a, velocity v, displacement u, impact force f, protection wall absorbed energy E_a were calculated. Velocity v is obtained by the time integration of acceleration a through the following formula.

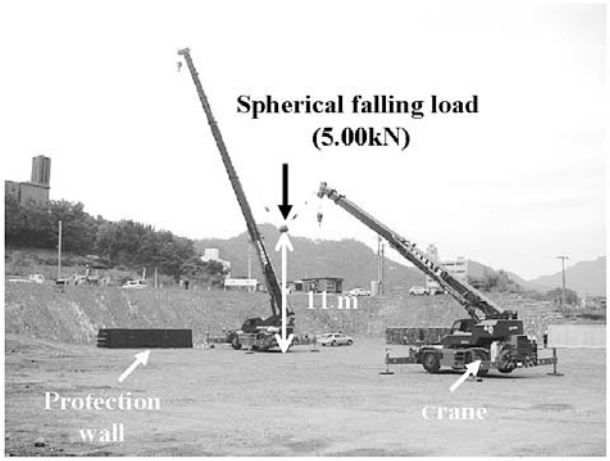

Photo 3 Experimental condition of the second-step field test

$$v = \int a dt \quad \cdots\cdots(1)$$

Falling weight displacement u is obtained by the time integration of falling weight velocity v, through the following formula.

$$u = \int v dt \quad \cdots\cdots(2)$$

The falling weight collision direction is considered as positive. The impact force is obtained by the product of acceleration a and weight m as shown in the following formula.

$$f = ma \quad \cdots\cdots(3)$$

Protection wall absorbed energy E_a is obtained by the time integration of the product of impact force f and displacement increment Δu:

$$E_a = \int f \Delta u dt \quad \cdots\cdots(4)$$

However, since displacement increment Δu is used, when the value of velocity v changes to negative, energy E_a absorbed by the protection wall is considered constant. Variations in the calculated values of various physical quantities over time are shown below.

In the second-step field test, in order to examine the perfor-

mance of the wall using a ductile cast iron panel, experiments were conducted on both a ductile cast iron panel and a geogrid-reinforced wall (**Photo 4**).

The geogrid-reinforced wall consists of impact catchment material, which directly catches rockfall and structurally distributes the impact force to an impact resistant structure, which responds to the transmitted power. Large bags made of high elastic textiles filled with similarly sized broken stones were used as the impact catchment material (soilbags). Although the filling material is not the most convenient, the bags constitute a flexible impact-absorbing layer. The resistant structure consists of horizontal layers of geogrid-reinforced soil of 500 mm in height. The geogrid-confined geomaterial resists the force distributed by the flexible impact catchment bag.

2.3 Third-step field test

In February 2007, real-scale field tests were carried out again in Kakamigahara. Experiments were performed at different impact points: 50 cm and 75 cm on a ductile cast iron panel wall and 50 cm and 125 cm on a new hybrid design wall combining wire mesh panel and ductile cast iron panel (**Photo 5**). The front face of the hybrid wall is made with a square cross-section wire mesh and the other faces with a ductile cast iron panel. After assembling the frame of the hybrid protection wall, it was filled up with the boulders in a similar way as the wall using ductile cast iron panel.

In this step of the field test, experiments were conducted in a similar way as in the second-step field test. A falling load energy of 100 kJ was used in this case as shown in **Fig. 4**. A 3-dimensional accelerometer was connected to the falling load and the calculation methods of velocity v, displacement u, impact force f, protection wall absorbed energy E_a are the same as those used in the second-step field test.

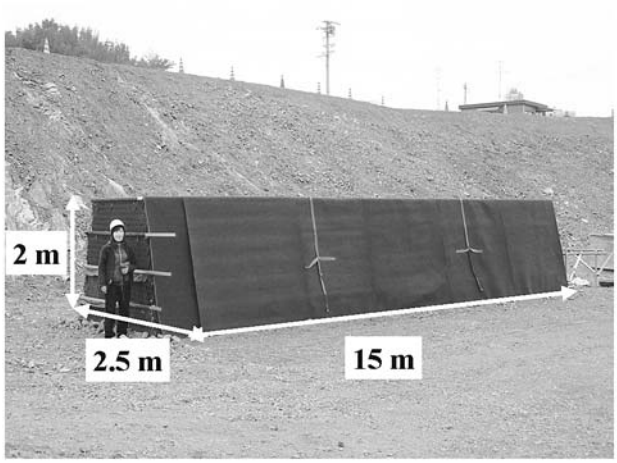

Photo 4 Geogrid-reinforced wall

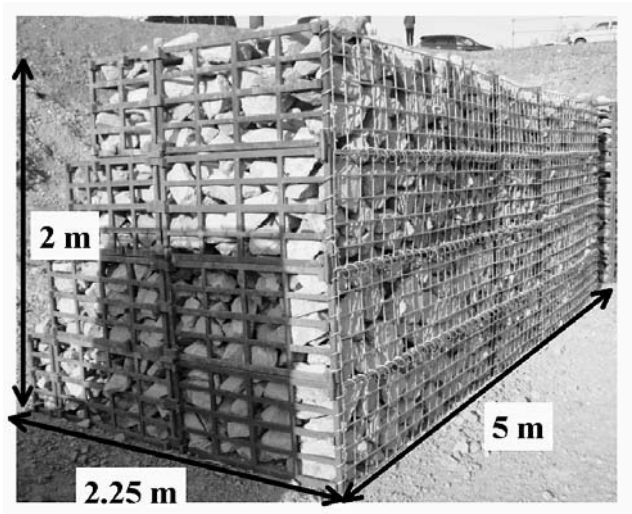

Photo 5 Hybrid wall combining wire mesh panel and ductile cast iron panel

3. EXPERIMENTAL RESULTS

Figs. 5 and **6** obtained from the first-step field test show the waveform of the impact force on the protection walls with and without panel frame shock absorbing material respectively. The maximum impact force shown in **Figs. 5** and **6** are obtained by adding the measurement of eight load cells installed in the back. The results obtained from several tests under the same condition are different because it was difficult to control the impact force due to friction between the mass and rough sloping ground (**Fig. 5**).

The analysis of **Fig. 6** where there is no panel frame shock absorbing material shows that the impact force is 10 times larger than that of **Fig. 5** where there is a panel frame shock absorbing material.

The impact waveform in the case where there is no panel frame shock absorbing material is very sharp and shows a large force at the time of collision, and the impact force dissipates in a short time. However, the dissipation time of the impact force is longer in the case with panel frame shock-absorbing material.

The relation between falling load weights and maximum values of the impact force are illustrated in **Fig. 7**. If the panel frame shock absorbing material is used, the impact force is very small, compared to that of the case where there is no panel frame shock absorbing material. After the impact test with the 0.36 kN load, collision marks were noticed on the panel frame as shown in **Photo 6**, however neither fracture nor remarkable damage was observed on the panel. Concerning the 1.67 kN load, the panel frame fractured after the first collision. Even after a second collision occurred at almost the same part, the damage range increased but

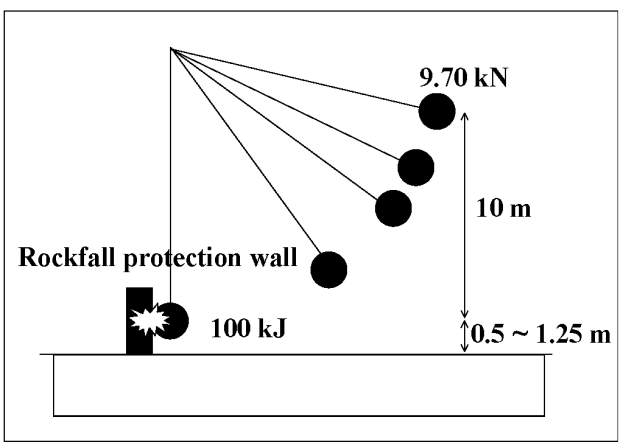

Fig. 4 Outline of the third-step field test

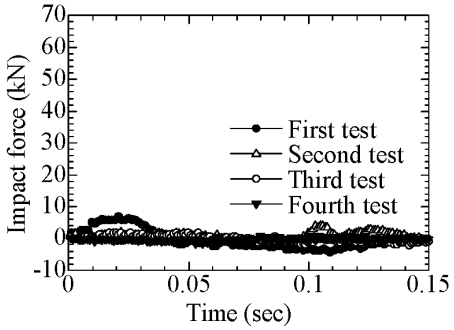

(a) 0.36 kN

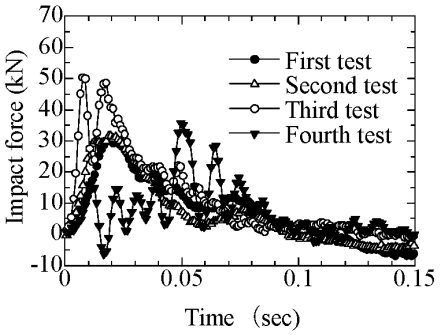

(b) 1.67 kN

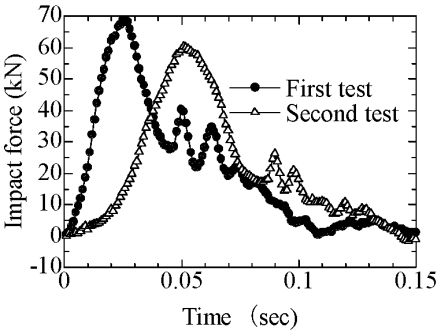

(c) 5.00 kN

Fig. 5 (a) 0.36 kN, (b) 1.67 kN, (c) 5.00 kN Waveform of the impact force (with ductile cast iron panel)

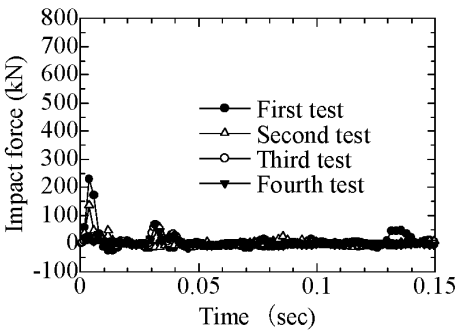

(a) 0.36 kN

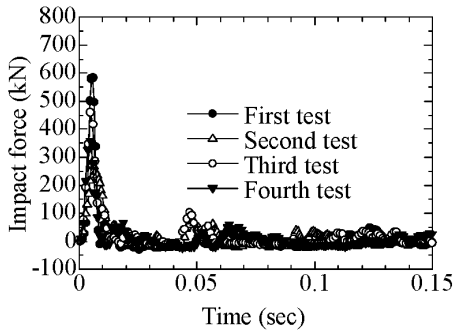

(b) 1.67 kN

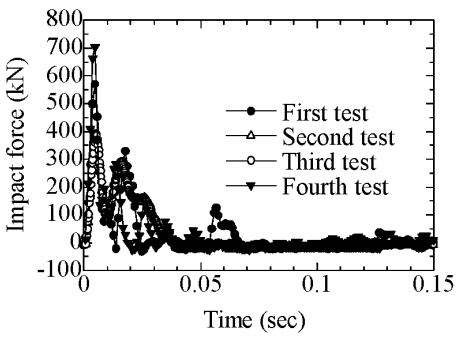

(c) 5.00 kN

Fig. 6 (a) 0.36 kN, (b) 1.67kN, (c) 5.00 kN Waveform of the impact force (without ductile cast iron panel)

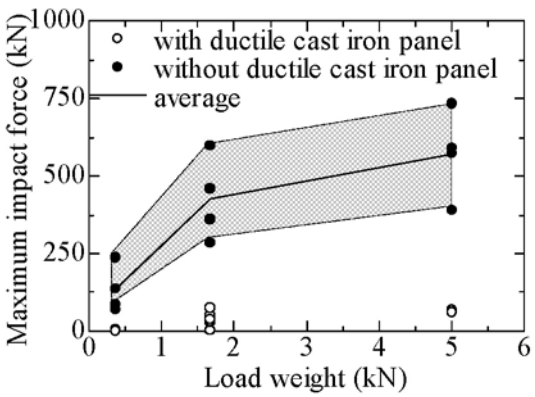

Fig. 7 Relation between load weight and maximum impact force

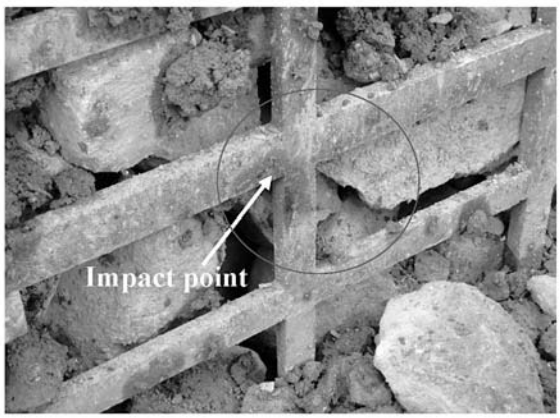

Photo 6 Panel after collision with 0.36 kN

the filling material remained intact and did not flow out (**Photo 7**). For the 5.00 kN load, although no fracture was noticed on the panel, the collided part curved at a depth of about 25 mm (**Photo 8**). In the case of the 1.67 kN load, the damage is smaller, because the kinetic energy was absorbed by the slope by bounding and sliding, when the load was slipping down.

Accordingly, the protection wall using cast iron panel and boulders is locally damaged by the rockfall. If the repairing method and the method of selecting the filling material are established, the protection wall using ductile cast iron panel can be used for low rockfall energy.

In the second-step field test, the results obtained from the protection wall using a ductile cast iron panel are compared with those of a geogrid-reinforced wall. The measured time of all the results shown below is 0.1 second after the collision time.

Fig. 8 and **Fig. 9** show respectively the variations per time of the acceleration and velocity of the falling loads used in the second-step field test. The variations in time of the barrier-absorbed energy and the impact force are given in **Fig. 10** and **Fig. 11**. The relation between the displacement and time after collision is shown in **Fig. 12**. The figures illustrate the results in the case of the geogrid-reinforced wall and the protection wall using a ductile cast iron panel.

The falling load acceleration shows a negative value after collision, and the velocity is decreasing accordingly (**Fig. 8** and **Fig. 9**). However, in the case of the geogrid-reinforced wall, the falling load acceleration has a higher value than the wall using the ductile cast iron panel, and the dissipation time of the acceleration is also shorter. Consequently, the velocity of the falling mass becomes negative in the early stage (**Fig. 9**), and the increase rate of the absorbed energy is also large (**Fig. 10**). This means that at this

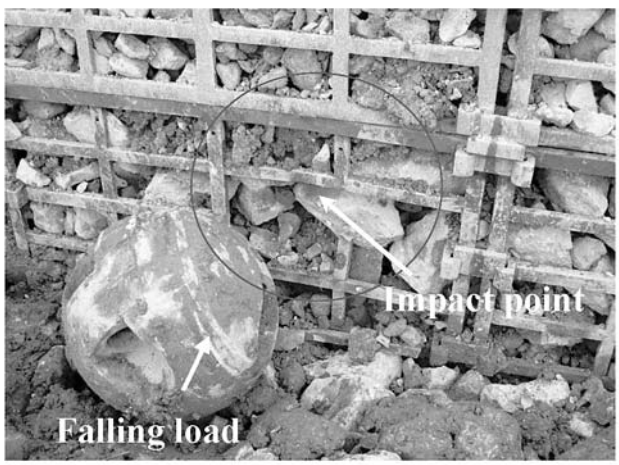

Photo 7 Panel after collision with 1.67 kN

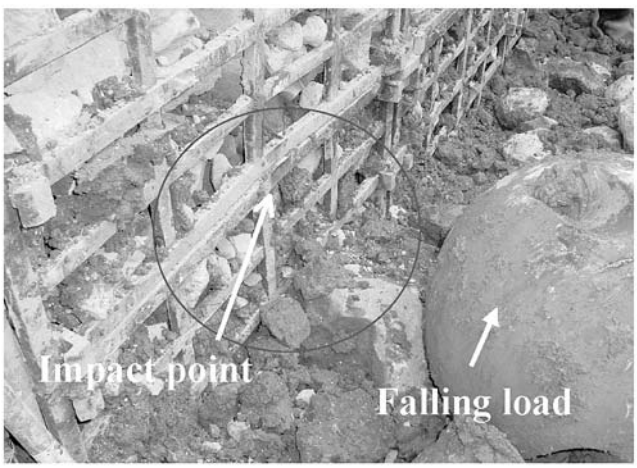

Photo 8 Panel after collision with 5.00 kN

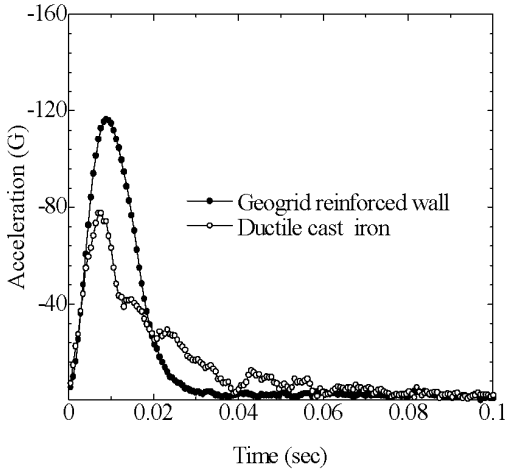

Fig. 8 Acceleration time history (tests in 2005)

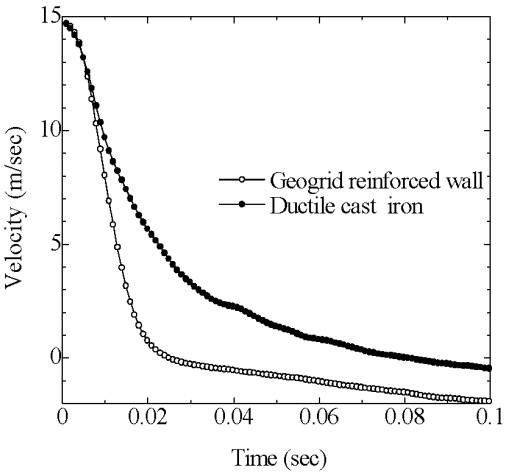

Fig. 9 Velocity time history (tests in 2005)

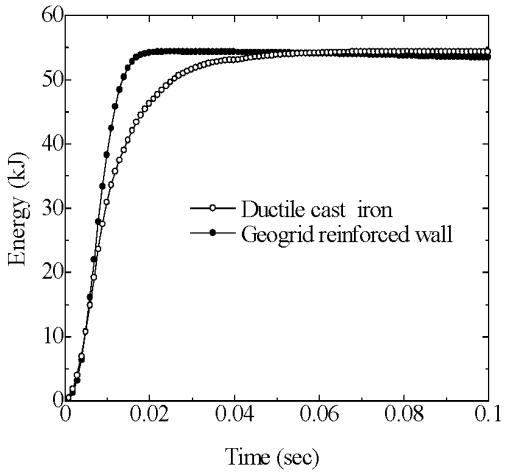

Fig. 10 Absorbed energy time history (tests in 2005)

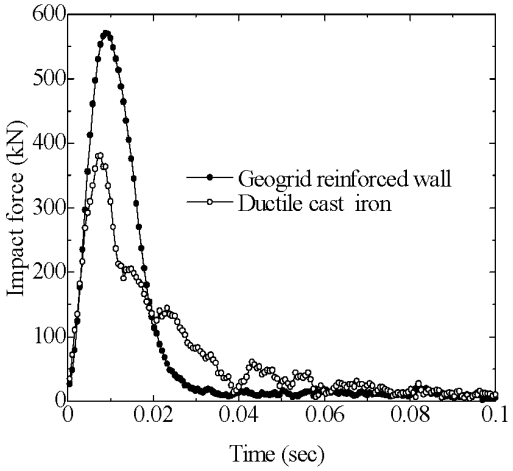

Fig. 11 Impact force time history (tests in 2005)

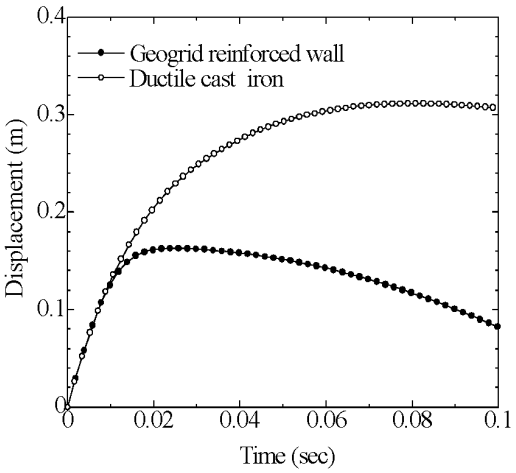

Fig. 12 Displacement time history (tests in 2005)

energy level, the geogrid-reinforced wall is stiffer than the wall using ductile cast iron panel.

The displacement-time relationship is illustrated in **Fig. 12**; the peak value expresses the maximum magnitude of penetration of the falling load but in the case of the geogrid-reinforced wall the peak value is smaller compared with the wall using ductile cast iron panel. This result also confirms the stiffness of the geogrid-reinforced wall. On the other hand, as the impact force is smaller and the deformation relatively larger for the ductile cast iron panel, the deformation of the whole structure at this energy level shows that the shock was effectively absorbed.

In the third-step field test, experiments were conducted with a falling weight of 9.70 kN and a fall height of 10.5 m. **Fig. 13** and **Fig. 14** show respectively the variations per time of the acceleration and velocity of the falling mass used in the third-step field test. The hybrid wall has the higher falling load acceleration than that of the ductile cast iron panel (**Fig. 13**). Consequently, the velocity of the falling mass changed in the early stage (**Fig. 14**), and the increase rate of the absorbed energy is also large (**Fig. 15**). This means that, the hybrid wall combining a wire mesh panel and ductile cast iron panel is stiffer than the wall using a ductile cast iron panel. The variation of the impact force is given in **Fig. 16**. **Fig. 17** shows the displacement-time relationship. The peak value,

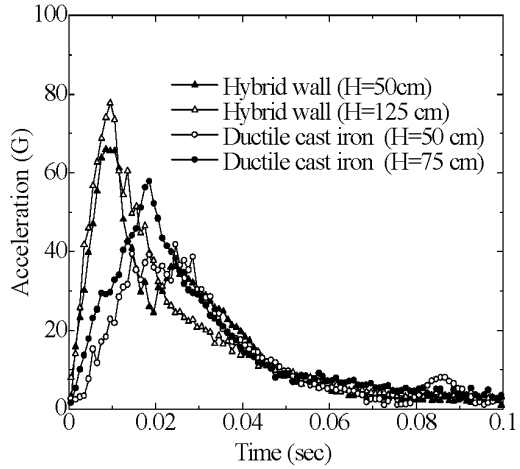

Fig. 13 Acceleration time history (tests in 2007)

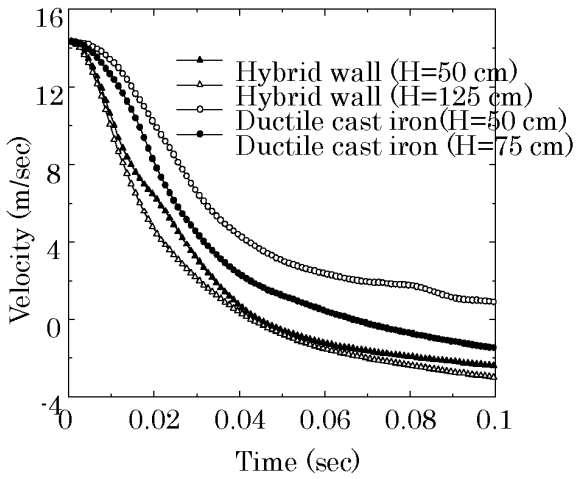

Fig. 14 Velocity time history (tests in 2007)

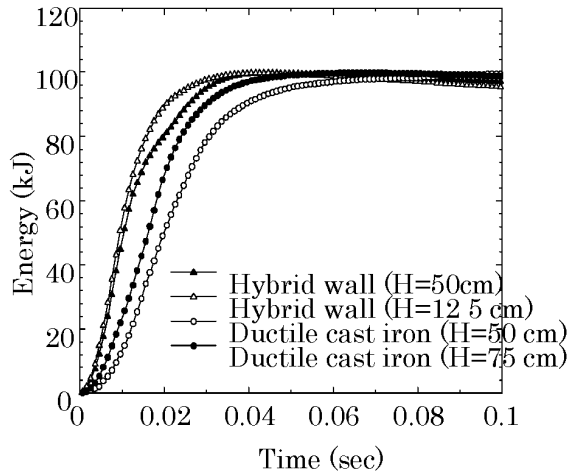

Fig. 15 Absorbed energy time history (tests in 2007)

which expresses the maximum magnitude of penetration of the falling load, is smaller in the case of the hybrid wall compared with the wall using a ductile cast iron panel. This result also confirms the stiffness of the hybrid wall.

Photos 9 and **10** show respectively the condition of the hybrid wall and the wall using ductile cast iron panel after collision. The

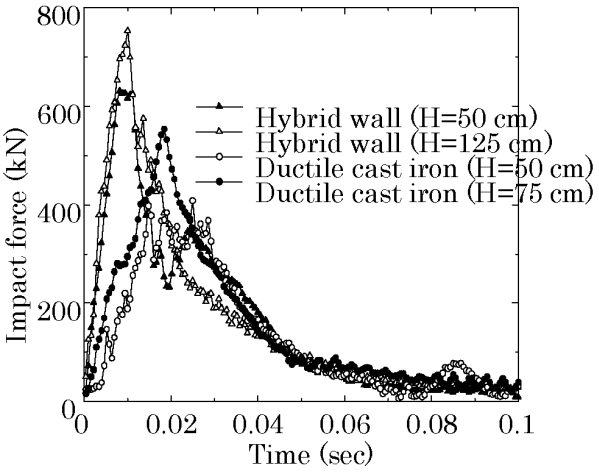

Fig. 16 Impact force time history (tests in 2007)

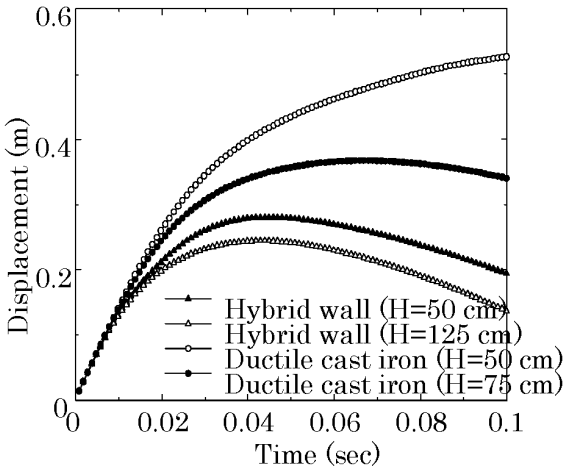

Fig. 17 Displacement time history (tests in 2007)

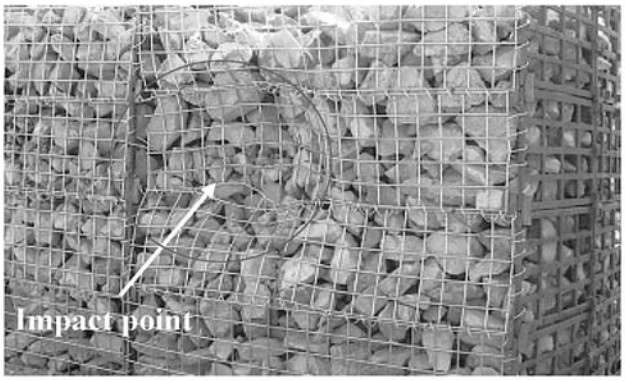

Photo 9 Hybrid wall after collision

Photo 10 Ductile cast iron panel after collision history (tests in 2007)

filling material of the hybrid wall remained intact and did not flow out (**Photo 9**).

The results obtained from the third-step field test show that the wall using ductile cast iron panel and the hybrid protection wall combining a wire mesh panel and cast iron panel are locally damaged by the falling load energy of 100 kJ. With a proper repairing method and material selection, the use of these types of protection wall is recommended.

4. CONCLUSION

This study shows the results of real-scale tests of the protection wall against rockfalls. Although there are few actual examples of application, the features of material configurations and their excellent performance as shock absorbers are demonstrated.

With the recent reductions in public investment, development and maintenance of the existing transportation network are essential. Therefore, it is important to identify economic and safe methods and, moreover, to develop a life cycle cost method for rockfall disaster prevention.

The main conclusions obtained from the tests are:

(1) Local material or surplus soil from other construction sites can be used. Recycling is possible.
(2) The barrier performs well and it has an efficient dissipative function.
(3) The proposed protection wall can be adjusted to the site geometry and the design and construction can take topographic features into account.
(4) Construction materials are mainly stone, so vegetation and planting are possible on the wall face.
(5) The type using ductile cast iron panels has very good permeability (its development can be expected). Considering the seepage effect of ductile cast iron panels, a hybrid design with other methods of construction is possible.
(6) A wall using ductile cast iron panels can be assembled swiftly (in two days) and less attention is required for the compaction and density when the panel is filled up with boulders. It can also be constructed even on soft ground without using rigid foundations.

Since the numbers of field tests are limited, numerical simulations with larger impacts will be carried out in the next step of this study series, in order to investigate the characteristic related-impact conditions such as stress and strain inside the structure. We will also propose methods of repairing damaged parts of the panels after collision with the falling load.

REFERENCES

Heierli, W., A. Merk and A. Temperli, 1981. Schutz gegen Steinschlag. Forschungsarbeit 6/80 auf Antrag der Vereinigung Schweizerischer

Straßenfachleute (VSS). Bundesamt für Straßenbau, Bern. 138 S.

Japan Road Association: Rock fall countermeasure manual, 2000.

Kobayashi, Y., E.L.Harp and T. Kagawa, 1990. Simulation of rockfalls triggered by earthquakes. Rock Mechanics and Rock Engineering, 23, 1-20.

Matsuo, O., I. Kenji, M. Hisashi 2002. Jap. Soc. of Geotechnical Engineering Vol.50 No.1 Ser. No.528 (in Japanese).

Matsuoka, N. and H. Sakai, 1999. Rockfall activity from an alpine cliff during thawing periods. Geomorphology, Vol. 28, 3, 309-328.

Sawada, K., S. Moriguchi, A. Yashima, M. Yoshida, N. Tatta, S. Inoue, Y. Nishida, T. Tatsui, Y. Nakagawa, T. Mutou, Y. Seno and T. Minowa, 2005. Real scale field tests of protective barrier for rock fall and soil flow utilizing features of geo-materials, Proceedings of the 14th Symposium on Investigation, Design and Construction Technology, Chubu Branch of JGS, pp.7-14(in Japanese).

Sumi, T. and A. Yashima, 2001., A method for extraction of the unstable wedge in rock slope considering water pressure and seismic force, Journal of Geotechnical Engineering, 687-56, pp. 125-138(in Japanese).

Ritchie, M., 1963. Evaluation of rockfall and its control, Highway Research Record, 17, pp.13-28.

Rochet, L., 1987. Application des modèles numériques de propagation a l'étude des éboulements rocheux. Bull Liaison Pont Chaussée 150/151, 84-95 (in French).

Yashima, A., K. Sawada, M. Goshima, S. Moriguchi, S. Inoue, Y. Nishida, T. Mutou, K Ueno and F. Kaneko, 2006., Real scale field tests of protective barrier for rock fall and soil flow utilizing features of geo-materials, Proceedings of the 15th Symposium on Investigation, Design and Construction Technology, Chubu Branch of JGS, pp.56-63 (in Japanese).